nature portfolio

https://doi.org/10.1038/s41563-021-00965-w

Supplementary information

Development of a photoelectrochemically self-improving Si/GaN photocathode for efficient and durable H_2 production

In the format provided by the
authors and unedited

Supplementary Information

Development of a photoelectrochemically self-improving Si/GaN photocathode for efficient and durable H_2 production

Guosong Zeng[1], Tuan Anh Pham[2], Srinivas Vanka[3], Guiji Liu[1], Chengyu Song[4], Jason K. Cooper[1], Zetian Mi[3*], Tadashi Ogitsu[2*], Francesca M. Toma[1,*]

1 Chemical Sciences Division, Lawrence Berkeley National Laboratory, 1 Cyclotron Road, Berkeley, California 94720, United States

2 Materials Science Division, Lawrence Livermore National Laboratory, 7000 East Avenue, Livermore, California 94550, United States

3 Department of Electrical Engineering and Computer Science, University of Michigan, 1301 Beal Avenue, Ann Arbor, Michigan 48109, United States

4 National Center for Electron Microscopy, The Molecular Foundry, Lawrence Berkeley National Laboratory, 1 Cyclotron Road, Berkeley, California 94720 United States

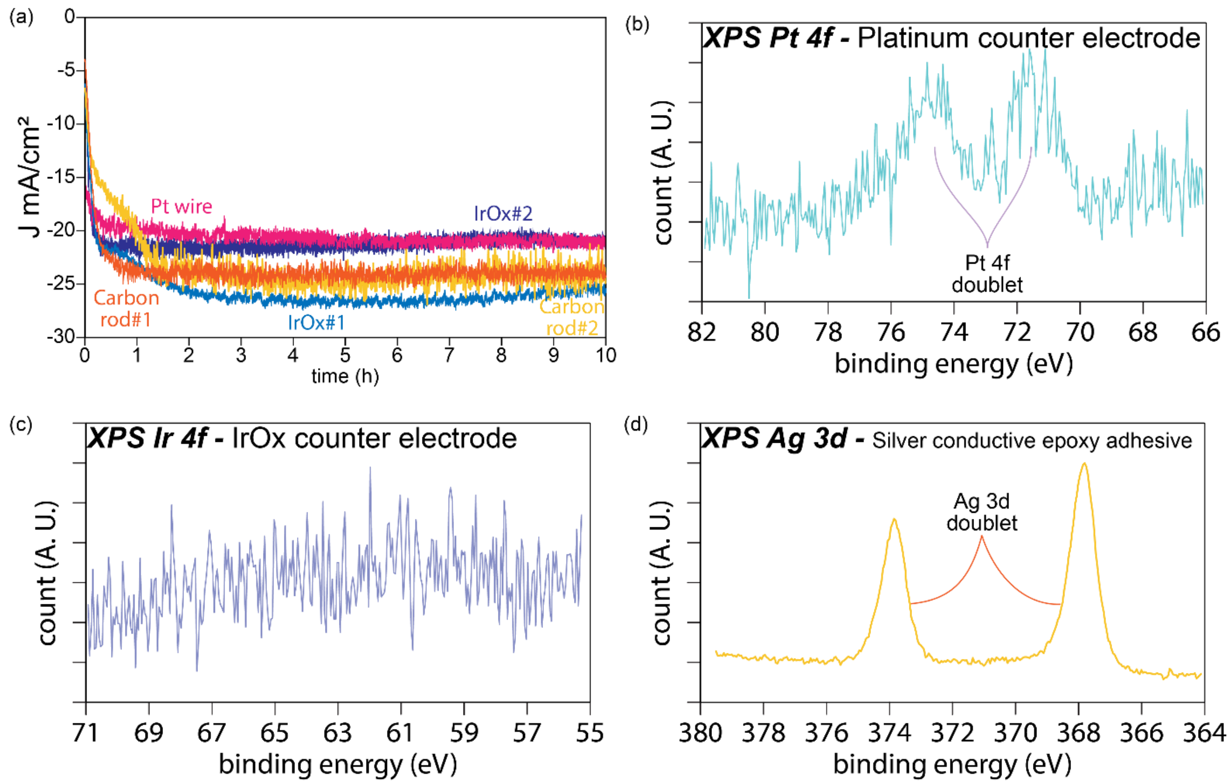

Fig. SI-1 Metal contamination verification. (a) J-T curves verify the self-improving behavior of GaN is independent of counter electrode; (b) XPS Pt 4f core level spectrum shows small amount of Pt transferred from Pt counter electrode to sample surface; (c) XPS Ir 4f core level spectrum shows no Ir contamination using IrOx as counter electrode; (d) XPS Ag 3d spectrum shows silver leakage and contaminates the sample surface when using Ag paste as conductive adhesive in electrode assembly.

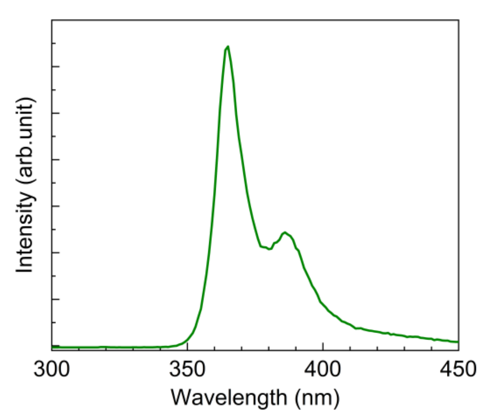

Fig. SI-2 PL of as-grown GaN quasi-epilayer on Si.

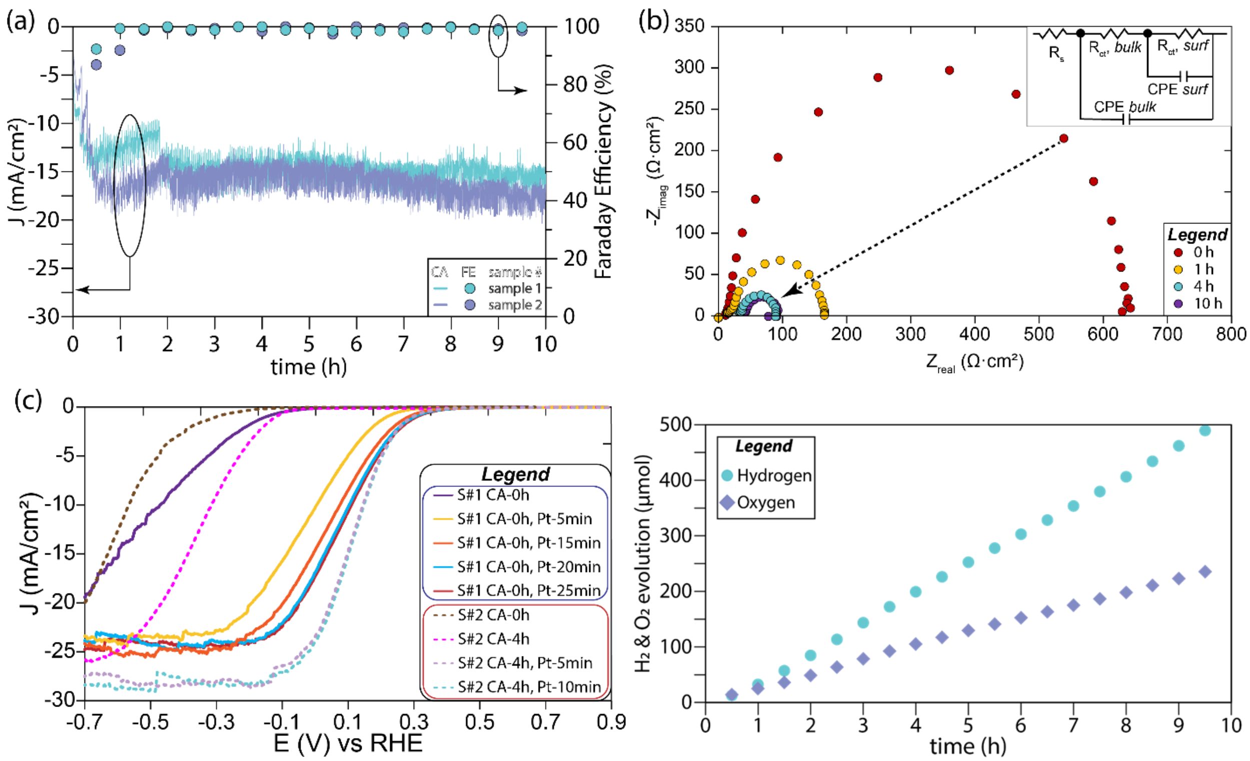

Fig. SI-3 (a) 10-hours CA testing under constant bias at -0.6 V vs RHE and the corresponding Faradaic efficiency also reveal a self-improvable nature of GaN as shown in Fig. 1b in the main text; (b) Electrochemical impedance spectra (EIS) analysis of Si/GaN photocathode as function of CA testing time. The experiment data is plotted in discrete points and the calculated results are listed in Table-S2. Inset shows the equivalent circuit obtained from the fitting; (c) J-E curves of as-prepared Si/GaN photocathode, 4 hours CA tested Si/GaN photocathode, and Si/GaN photocathode with different Pt photodeposition duration under 1 sun illumination; (d) Gas product measured by gas chromatography (GC).

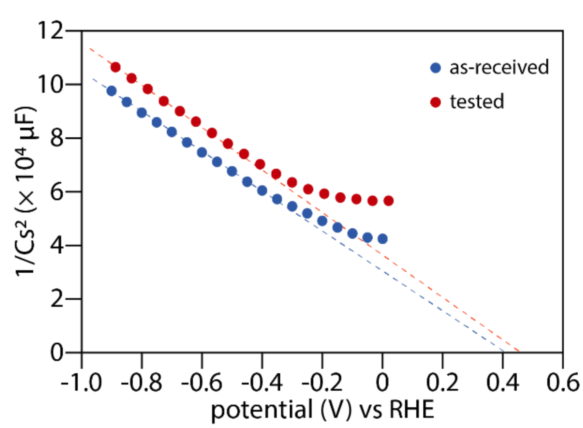

Fig. SI-4 Mott-Schottky curves for as-received Si/GaN photocathode and CA tested Si/GaN photocathode. The extrapolations of these curves show similar flat band potentials before and after the CA testing.

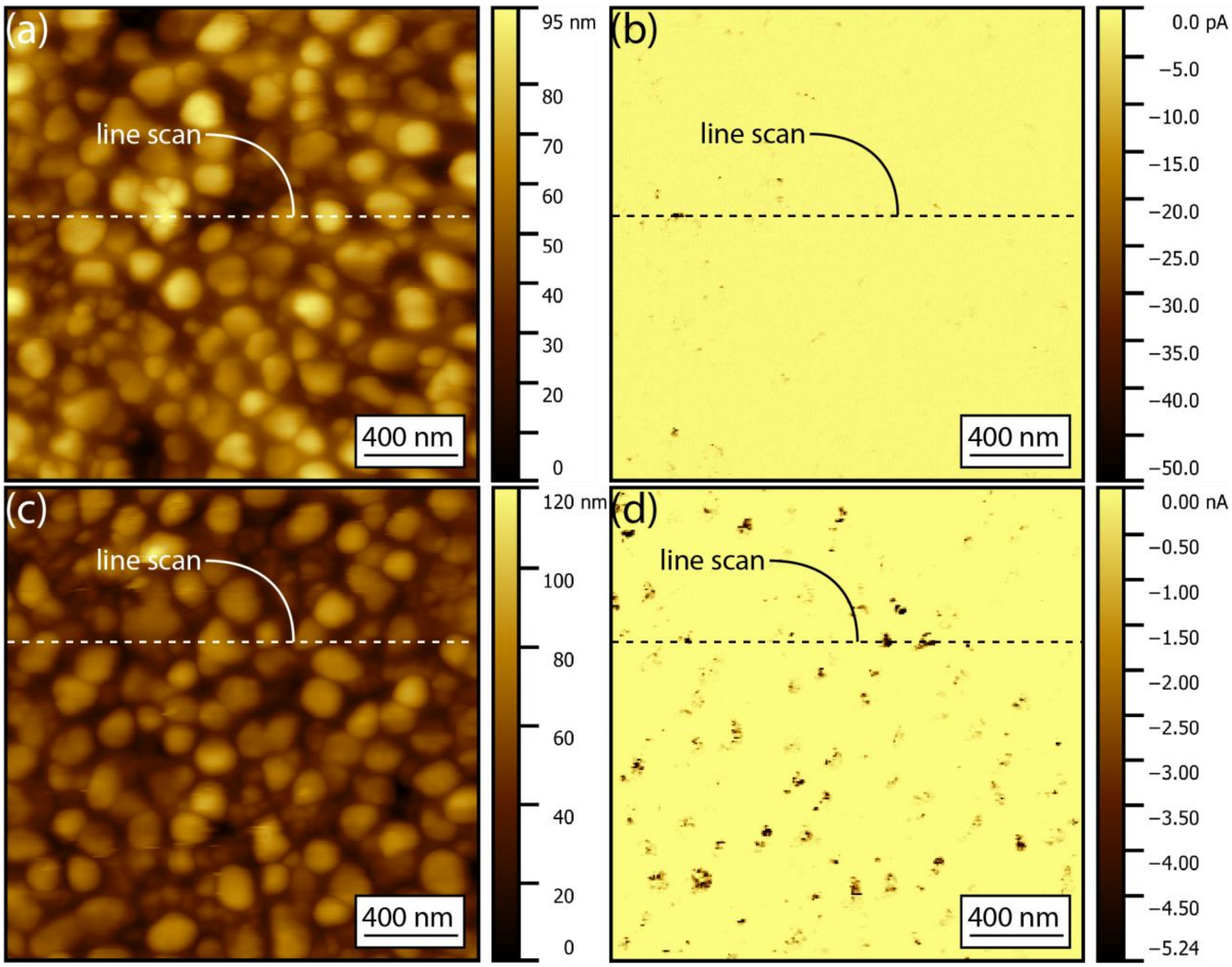

Fig. SI-5 pc-AFM characterization on CA-0h and CA-10h surfaces. Left hand side shows the morphology of the (a) CA-0h sample and (c) CA-10h sample, the right-hand side shows the corresponding photocurrent mappings measured under illumination (b) CA-0h and (d) CA-10h samples. Line scans on each sample refer to the extracted profiles presented in Fig. 2.

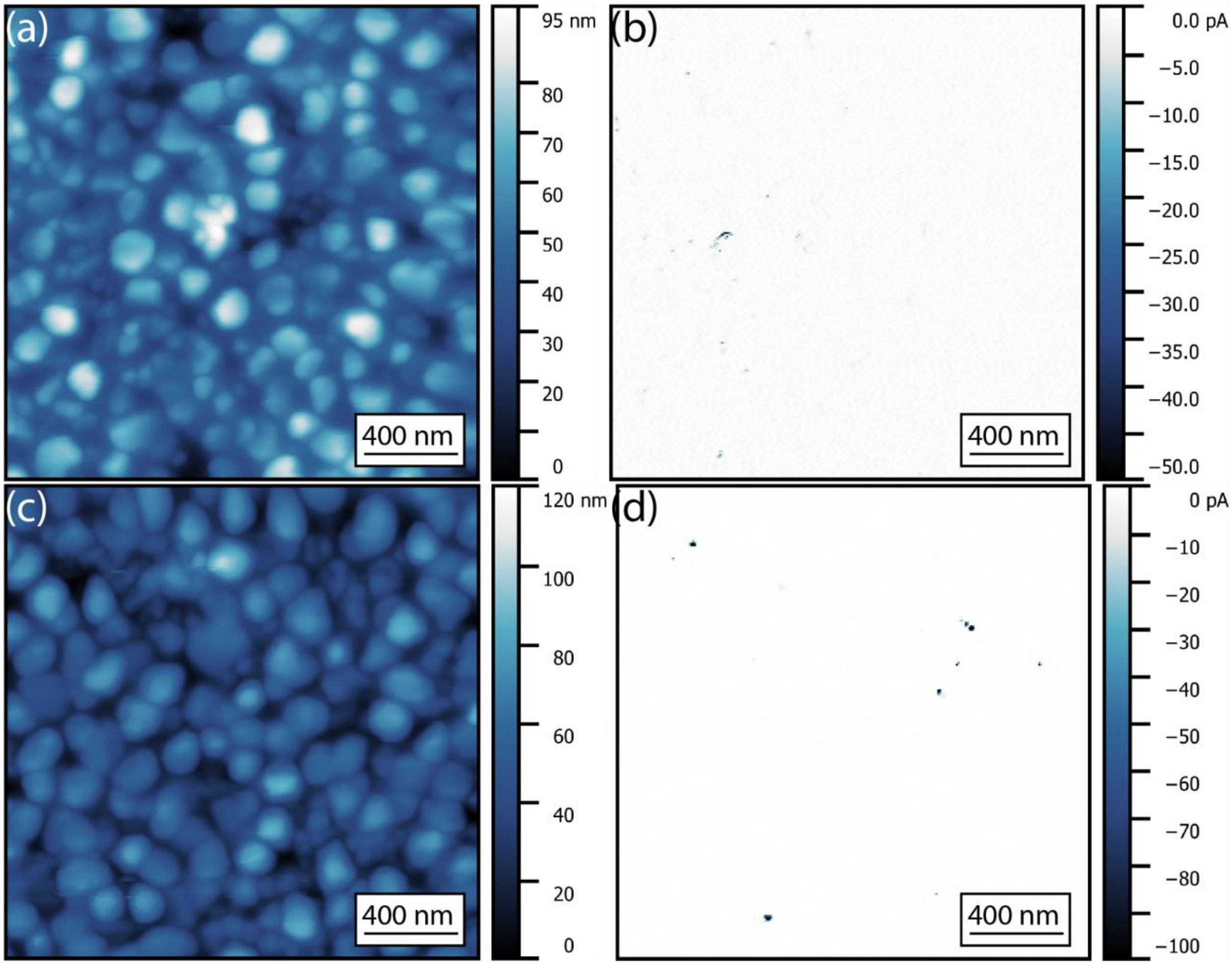

Fig. SI-6 (a) and (b) show the morphology and dark current of CA-0h sample, respectively; (c) and (d) show the morphology and dark current of CA-10h sample. The dark current showed here is negligible when compared to the photocurrent in Fig. SI-2.

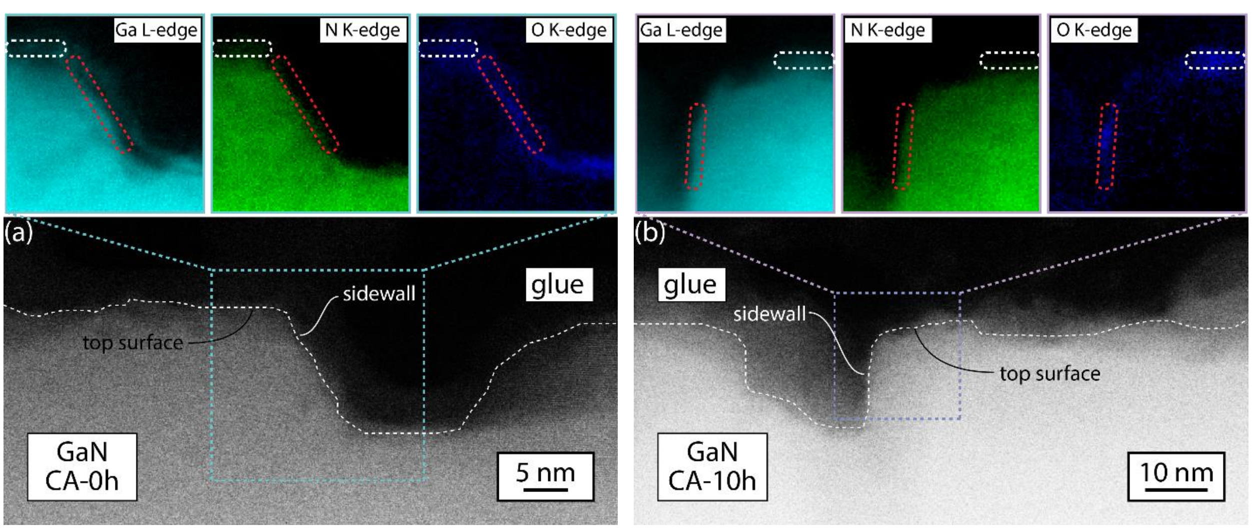

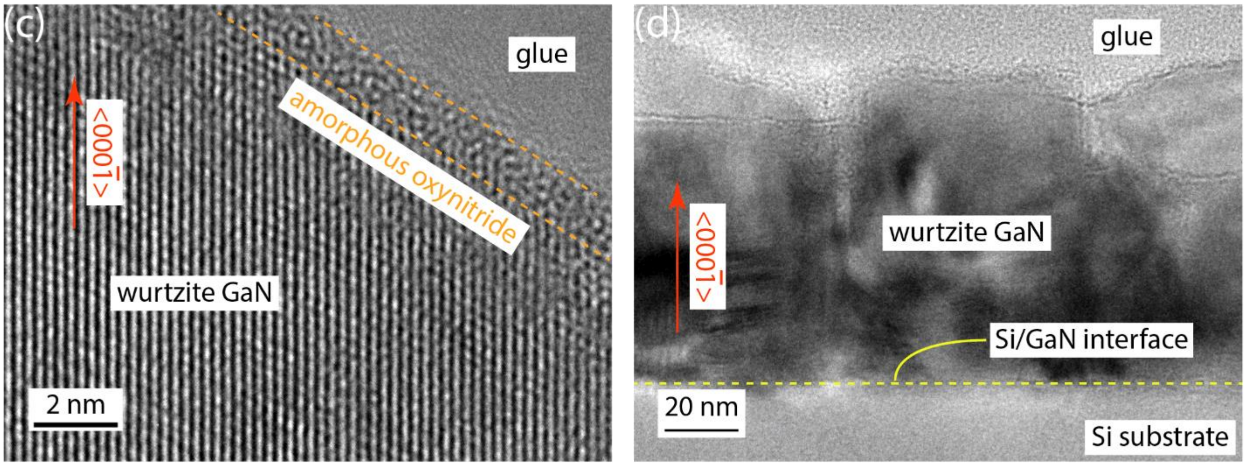

Fig. SI-7 Additional STEM/EELS to verify the existing of oxynitride formation on the sidewall of GaN after PEC testing: (a) STEM image of as-prepared surface with insets (left to right) showing the EELS mappings of Ga L-edge, N K-edge and O K-edge; (b) STEM image of CA-10h surface with insets (left to right) showing the EELS mappings of Ga L-edge, N K-edge and O K-edge; (c) HRTEM showing a thin amorphous layer of oxynitride on the sidewall of GaN grain while the main crystal structure of GaN still remains as wurtzite structure; (d) TEM image shows the interface of quasi-epilayer of GaN and Si substrate.

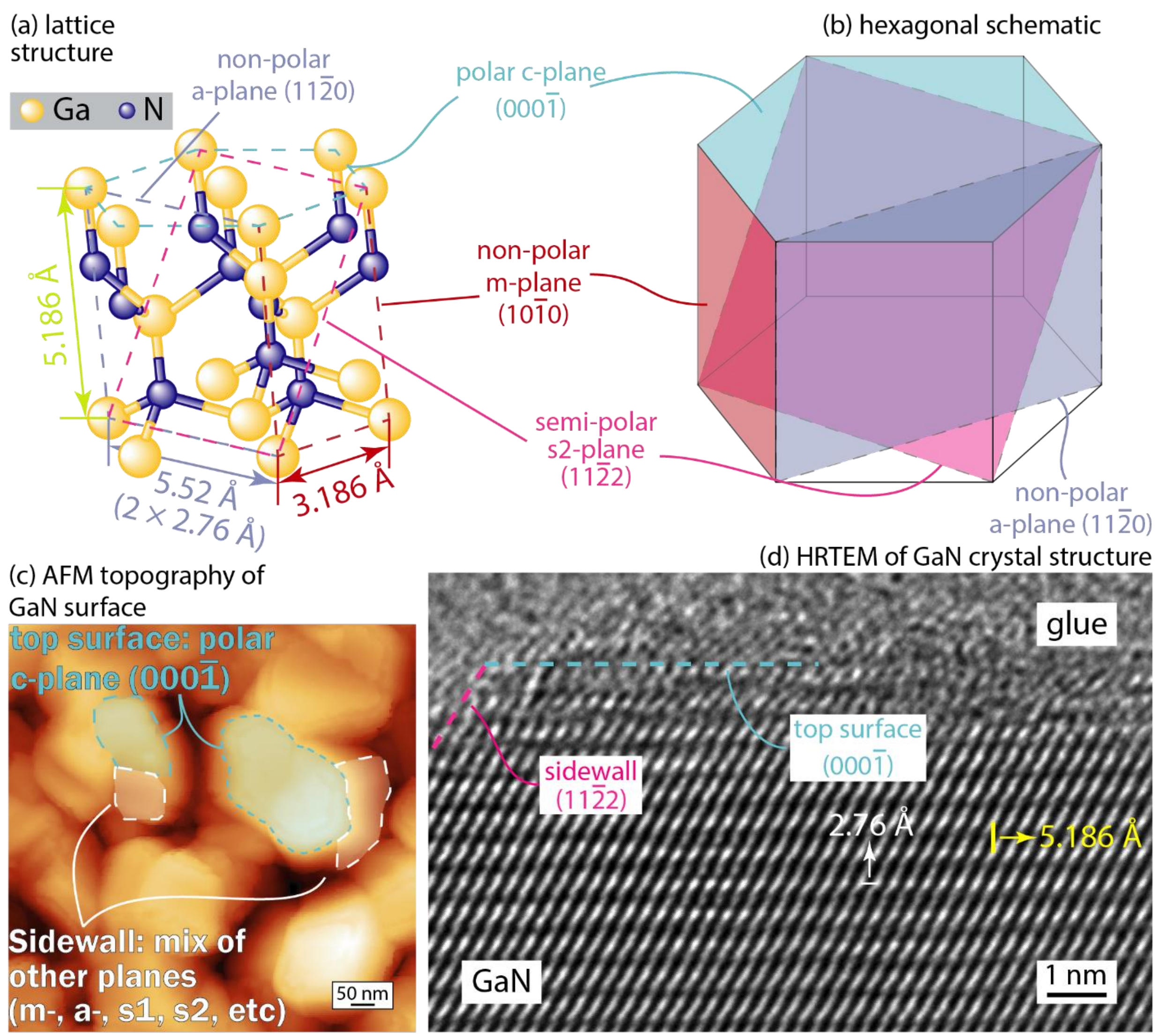

Fig. SI-8 Illustration of GaN wurtzite structure. (a) wurtzite lattice structure of GaN, with polar c-plane on top and non-polar m- and a-planes on the side; (b) hexagonal schematic of GaN wurtzite structure; (c) assigning the crystal planes to the actual GaN grains, with top surface of the grains are c-plane, the sidewall of the grains are mixed of other planes; (d) HRTEM reveals the crystal structure of MBE-grown GaN used in this study.

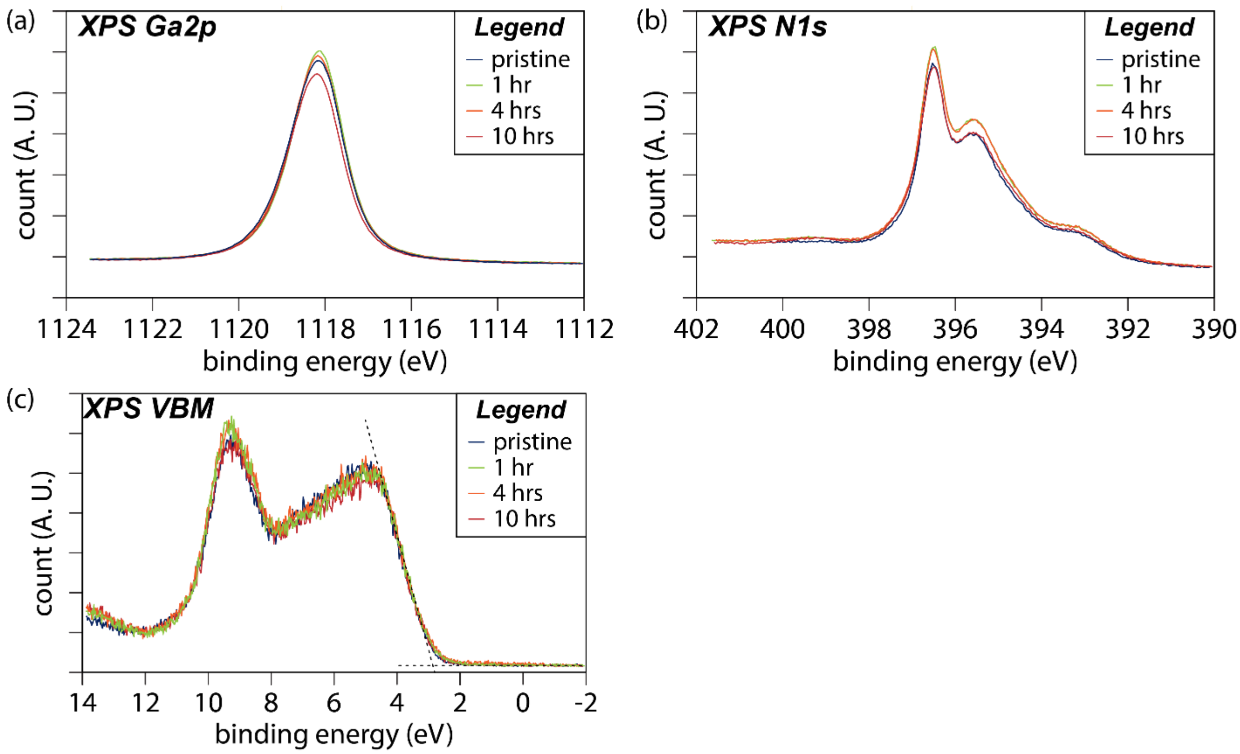

Fig. SI-9 (a) Ga *2p*, (b) N *1s* and (c) VBM spectra of CA-0h, CA-1h, CA-4h and CA-10h samples. The Ga *2p* and N *1s* core level spectra as well as VBM show similar profile regardless of testing time, indicating that within the probing depth of the XPS, the material is still dominated by GaN.

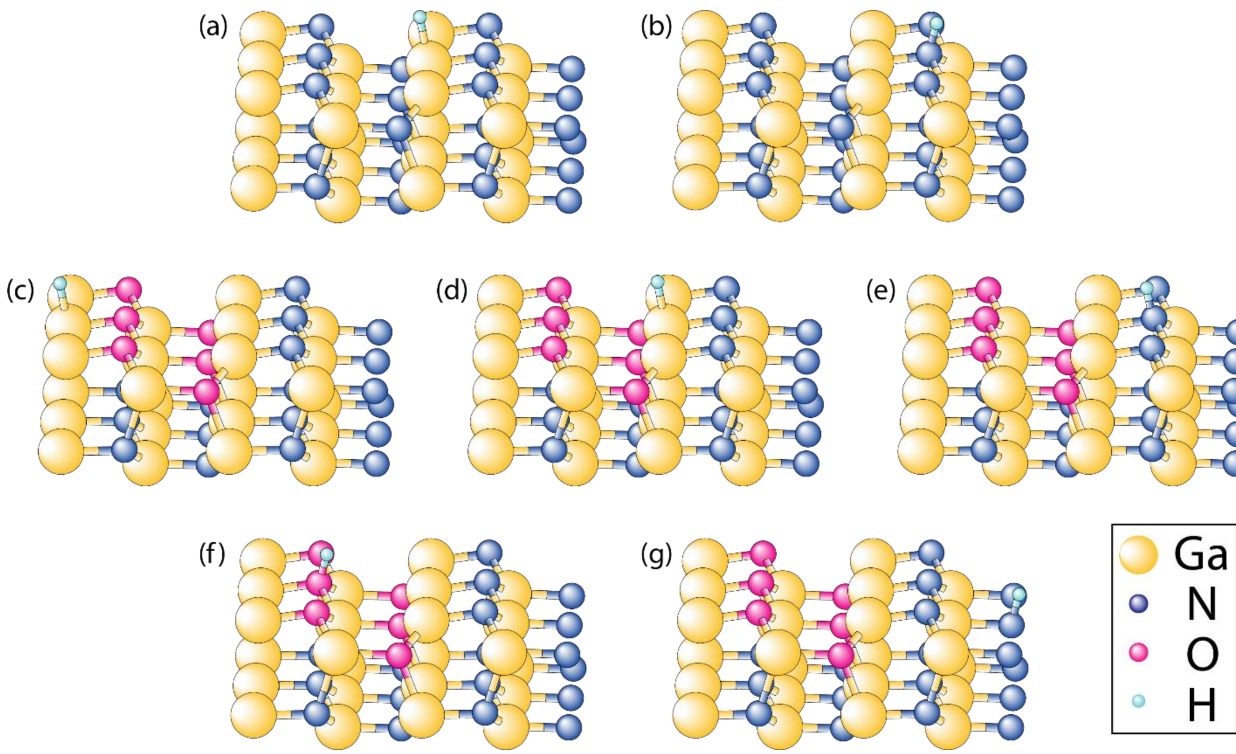

Fig. SI-10 Schematic of DFT configurations for free energy calculation. (a) ideal m-plane GaN with a hydrogen atom bonding to a gallium atom; (b) ideal m-plane GaN with a hydrogen atom bonding to a nitrogen atom; (c) gallium oxynitride forming at m-plan GaN with a hydrogen atom bonding to a gallium atom that associated with oxygen; (d) gallium oxynitride forming at m-plan GaN with a hydrogen atom bonding to a gallium atom that associated with nitrogen; (e) gallium oxynitride forming at m-plan GaN with a hydrogen atom bonding to a nitrogen atom; (f) gallium oxynitride forming at m-plan GaN with a hydrogen atom bonding to an oxygen atom; (g) gallium oxynitride forming at m-plan GaN with a hydrogen atom bonding to a subsurface nitrogen atom.

Table S-1 Comparison of up-to-date record efficiencies as well as the device stability of protected Si-photocathodes

Materials	Electrolyte	catalyst	Stability	Illumination	Onset potential (vs RHE)	Reference
MoS_2/MnO/n^+p Si photocathode	0.5 M H_2SO_4	MoS_2	1440 h	1 sun	0.28 V	Ref [1]
NiMo/NiSi/n^+p Si MW photocathode	1 M KOH	Pt	288 h	1 sun	0.55 V	Ref [2]
Pt (1nm)/TiO_2/Ti/ n^+-p Si photocathode	0.5 M H_2SO_4	Pt	300 h	1 sun	0.64 V	Ref [3]

Pt NPs/TiO_2/Ti/n^+-p Si photocathode	1 M $HClO_4$	Pt	720 h	1 sun	0.35 V	Ref [4]
Pt/n-GaN/n^+p Si photocathode	0.5 M H_2SO_4	Pt	3000 h	1 sun	0.56 V	Ref [5]
nano-MoS_2 layer on Al_2O_3/n^+p-Si photocathode	$HClO_4$	MoS_2	120 h	1 sun	0.4 V	Ref [6]
TiO_2/Pt/n^+p-Si photocathode	$HClO_4$	Pt	168 h	1 sun	0.6 V	Ref [7]
Pt (2nm)/SiHJ	1 M H_2SO_4	Pt	10 h	1 sun	0.64 V	Ref [8]
Pt-Al_2O_3-Nanoporous-pSi	0.5 M H_2SO_4	Pt	12 h	1 sun	0.05 V	Ref [9]
$MoSe_2$/n^+p Si (Textured)	1 M $HClO_4$	$MoSe_2$	120 h	1 sun	0.4 V	Ref [10]
n-GaN quasi-epilayer/n^+p Si photocathode	0.5 M H_2SO_4	No catalyst	150 h	3.5 suns	Initial: -0.46 V Self-improved: -0.08 V	This work

Table S2: Change of onset potential (E_{onset}) at different time points

	CA-0h	*CA-1h*	*CA-2h*	*CA-3h*	*CA-4h*	*CA-6h*	*CA-8h*	*CA-10h*
E_{onset} (mV)	-460	-280	-270	-240	-170	-150	-120	-80

Table S3: Resistance comparison of as-prepared, CA tested after 1hr, CA tested after 4hrs and CA tested for 10hrs samples

	R_s	***R_{ct}, bulk***	***R_{ct}, surface***	***CPE surface***	***CPE bulk***
CA-0h	10.24	16.67	611.5	1.53×10^{-6}	1.33×10^{-6}
CA-1h	11.97	17.56	136.7	1.94×10^{-6}	1.73×10^{-6}
CA-4h	17.42	15.32	109.2	2.41×10^{-6}	6.90×10^{-7}
CA-10h	17.39	18.21	104.7	3.05×10^{-6}	7.33×10^{-7}

Reference

1. King, L. A., Hellstern, T. R., Park, J., Sinclair, R. & Jaramillo, T. F. Highly Stable Molybdenum Disulfide Protected Silicon Photocathodes for Photoelectrochemical Water Splitting. *ACS Appl. Mater. Interfaces* **9**, 36792–36798 (2017).

2. Vijselaar, W., Tiggelaar, R. M., Gardeniers, H. & Huskens, J. Efficient and stable silicon microwire photocathodes with a nickel silicide interlayer for operation in strongly alkaline solutions. *ACS energy Lett.* **3**, 1086–1092 (2018).

3. Ros, C. *et al.* Charge Transfer Characterization of ALD-Grown TiO2 Protective Layers in Silicon Photocathodes. *ACS Appl. Mater. Interfaces* **9**, 17932–17941 (2017).

4. Seger, B. *et al.* Silicon protected with atomic layer deposited TiO2: Durability studies of photocathodic H2 evolution. *RSC Adv.* **3**, 25902–25907 (2013).

5. Vanka, S. *et al.* Long-term stability studies of a semiconductor photoelectrode in three-electrode configuration. *J. Mater. Chem. A* **7**, 27612–27619 (2019).

6. Fan, R. *et al.* Efficient and Stable Silicon Photocathodes Coated with Vertically Standing Nano-MoS2 Films for Solar Hydrogen Production. *ACS Appl. Mater. Interfaces* **9**, 6123–6129 (2017).

7. Fan, R., Dong, W., Fang, L., Zheng, F. & Shen, M. More than 10% efficiency and one-week stability of Si photocathodes for water splitting by manipulating the loading of the Pt catalyst and TiO 2 protective layer. *J. Mater. Chem. A* **5**, 18744–18751 (2017).

8. Wang, H.-P. *et al.* High-performance a-Si/c-Si heterojunction photoelectrodes for photoelectrochemical oxygen and hydrogen evolution. *Nano Lett.* **15**, 2817–2824 (2015).

9. Choi, M. J. *et al.* Long-term durable silicon photocathode protected by a thin Al 2 O 3/SiO x layer for photoelectrochemical hydrogen evolution. *J. Mater. Chem. A* **2**, 2928–2933 (2014).

10. Huang, G. *et al.* Integrated MoSe2 with n+ p-Si photocathodes for solar water splitting with high efficiency and stability. *Appl. Phys. Lett.* **112**, 13902 (2018).